# Monolithically integrated InP 1 x 16 optical switch with wavelength-insensitive operation

# Monolithically Integrated InP 1 × 16 Optical Switch With Wavelength-Insensitive Operation

Ibrahim Murat Soganci, *Student Member, IEEE*, Takuo Tanemura, Kevin A. Williams, Nicola Calabretta, Tjibbe de Vries, E. Smalbrugge, Meint K. Smit, Harm J. S. Dorren, and Yoshiaki Nakano, *Member, IEEE*

***Abstract*—The static and dynamic characteristics of a monolithically integrated InP 1 × 16 optical phased-array switch are presented. The device demonstrates static switching with an average extinction ratio of 18.6 dB, on-chip loss below 7 dB, and wavelength dependence of less than 0.8 dB in the entire $C$-band. A 40-Gb/s nonreturn-to-zero signal is transmitted through the switch with a power penalty below 0.4 dB. Using a programmable electronic circuit, dynamic switching to all 16 outputs is achieved with response times less than 11 ns.**

***Index Terms*—Integrated photonics, optical packet switching (OPS), optical switches, phased arrays.**

## I. Introduction

POWER-HUNGRY and high-cost electronic switching is expected to be a bottleneck while scaling the capacity of communication networks. Optical packet switching (OPS) is a possible solution thanks to its transparency and high network utilization efficiency under dynamically changing traffic conditions [1]. In particular, wavelength-division-multiplexed OPS (WDM-OPS) can achieve ultrahigh throughput with relatively small-scale switches [2], [3]. Several optical functions are necessary for WDM-OPS, including high-speed and wavelength-insensitive optical switches. Compound semiconductor photonic integrated circuits are attractive to implement monolithic integration of active and passive devices with low cost, small footprint, and low power consumption [4]. However, the port counts of integrated compound semiconductor photonic switches have been limited so far [5], [6]. Insertion loss, power consumption, excess noise, footprint, and complexity of design and fabrication become technical problems as the port count increases. To overcome these problems, we have recently introduced the phased-array scheme in high-speed integrated optical switching [7]–[9]. Because of its single-stage, all-passive architecture, the phased-array switch is expected to be highly scalable in terms of the number of ports [10]

Manuscript received September 22, 2009; revised November 02, 2009; accepted November 07, 2009. First published November 24, 2009; current version published January 13, 2010. This work was supported by Grant-in Aid for Scientific Research (S) #20226008, Japan Society for the Promotion of Science. The photomasks were fabricated using the 8-in EB writer F5112 + VD01 (donated by ADVENTEST Corporation) of the University of Tokyo VLSI Design and Education Center (VDEC).

I. M. Soganci, T. Tanemura, and Y. Nakano are with the Research Center for Advanced Science and Technology, University of Tokyo, Tokyo 153-8904, Japan (e-mail: imsoganci@hotaka.t.u-tokyo.ac.jp; tanemura@ee.t.u-tokyo.ac.jp; nakano@ee.t.u-tokyo.ac.jp).

K. A. Williams, N. Calabretta, T. de Vries, E. Smalbrugge, M. K. Smit, and H. J. S. Dorren are with COBRA Research Institute, Eindhoven University of Technology, 5600 MB Eindhoven, The Netherlands (e-mail: K.A.Williams@tue.nl; N.Calabretta@tue.nl; t.d.vries@tue.nl; e.smalbrugge@tue.nl; M.K.Smit@tue.nl; hdorren@tue.nl).

Color versions of one or more of the figures in this letter are available online at http://ieeexplore.ieee.org.

Digital Object Identifier 10.1109/LPT.2009.2036859

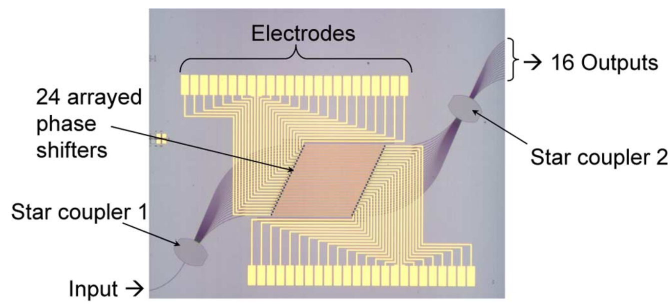


Fig. 1. Micrograph of the 1 × 16 optical switch. The total device size is 4.1 mm × 2.6 mm, including the input/output bends and lateral tapers, which are not completely shown in the figure. The waveguides are facet normal at the input and the outputs.

In this letter, we investigate the basic characteristics of the monolithically integrated InP 1 × 16 optical switch to verify the scalability of optical phased-array scheme. Broadband switching to all 16 outputs is demonstrated over the entire $C$-band with a wavelength dependence less than 0.8 dB. Additionally, we achieve complete dynamic operation of the device using a programmable electronic circuit for the first time.

## II. Design and Fabrication of the Optical Switch

The switch is entirely integrated on an InP substrate in a guided-wave fashion and consists of three parts separated by two star couplers. There are 24 waveguides with 800-$\mu$m-long phase shifters at the array plane between the star couplers, in addition to one input waveguide and 16 output waveguides. Fig. 1 shows the micrograph of the fabricated device. Switching is achieved by applying electrical signal to the phase shifters independently to control the interference pattern at the output plane. Linear phase distribution (with modulo $2\pi$) at the array plane causes a tilt of the wavefront at the input of the second star coupler, resulting in beam deflection.

The lateral dimensions were chosen to achieve moderate device size and propagation loss in the straight and bent waveguides. The width of the passive waveguides is 2 $\mu$m while that of the phase shifters is 3.5 $\mu$m. The minimum radius of curvature of the bends is 500 $\mu$m. The length of the star couplers is 240 $\mu$m. At the interfaces to the star couplers, the pitches of the arrayed waveguides and the output waveguides are 2.5 and 2.8 $\mu$m, respectively. The total dimensions of the device are 4.1 mm × 2.6 mm including the input and output bends and the lateral tapers for better fiber coupling.

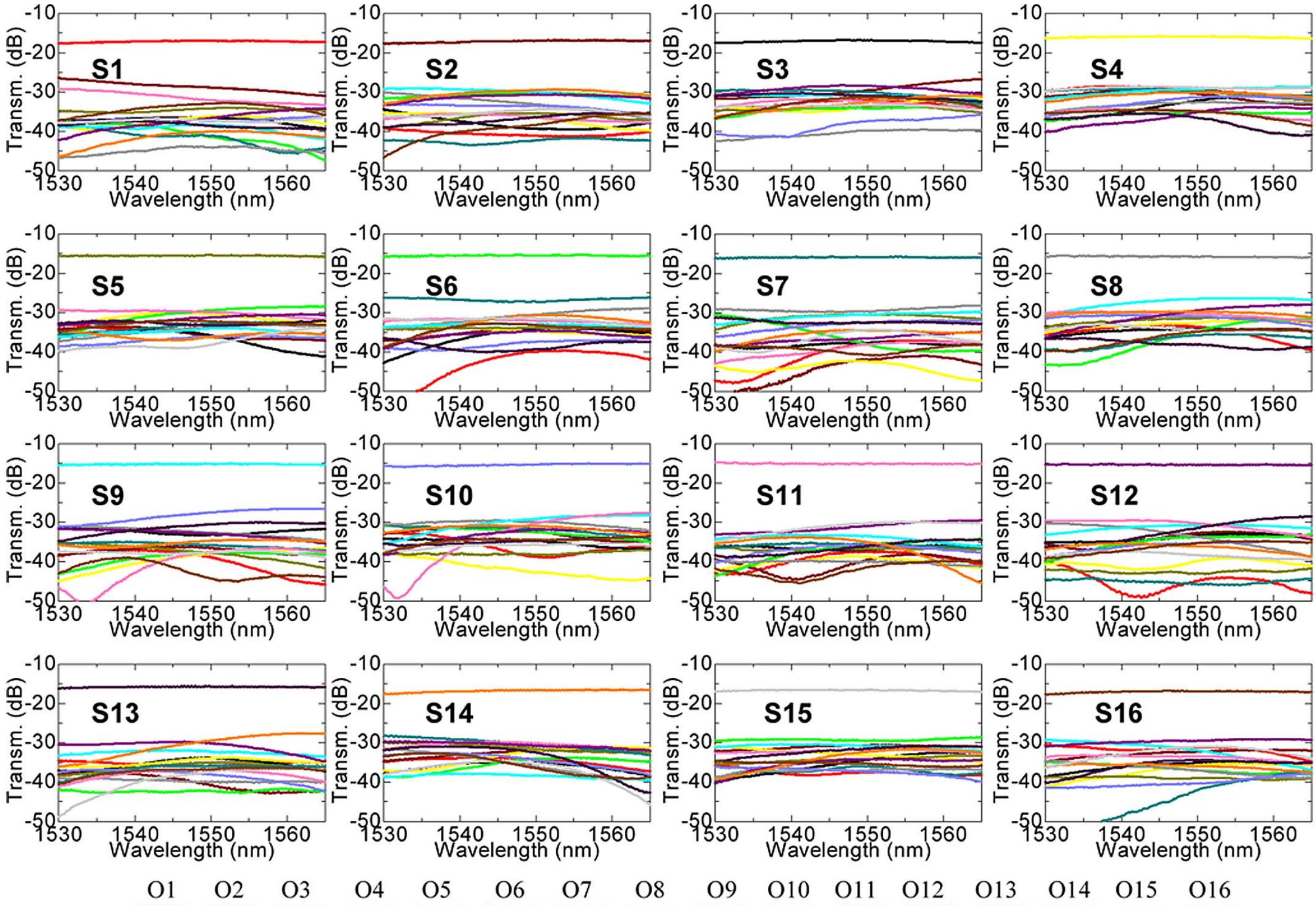


Fig. 2. Fiber-to-fiber optical transmissivity at the outputs in the States 1 to 16 (S1–16) in the $C$-band. The transmissivity spectra are averaged over bands of 100 pm to eliminate the Fabry–Pérot oscillation (period $\approx$ 60 pm) for clear view. The on-chip loss is estimated to be less than 7 dB at 1550-nm wavelength in all the states.

The entire chip has an identical epitaxial structure of p-i-n InP–InGaAsP double heterojunction fabricated by single metal–organic vapor phase epitaxy (MOVPE) growth. The guiding layer consists of 500-nm-thick undoped, bulk InGaAsP that has a photoluminescence peak at 1.3-$\mu$m wavelength (Q1.3). A 200-nm-thick undoped InP layer was inserted in between the InGaAsP core and the p-InP upper cladding layers to reduce the propagation loss. The waveguides and the star couplers were formed by single-step shallow reactive ion etching (RIE). After waveguide formation, the fabrication process was completed by subsequent steps of polyimide deposition for planarization and electrical isolation, contact opening, and electrodes formation by Pt–Ti–Au deposition followed by lift-off. After annealing the sample for Ohmic contact and thinning its substrate, we diced the individual devices and located them on aluminum nitride chip carriers. The phase shifters were wire bonded to the electrodes on the chip carrier.

## III. Experimental Results

We first derived the operating conditions of the phase shifters to switch to individual output ports by using continuous-wave (CW) light with a wavelength of 1550 nm. The switch operates in 16 states, each optimized to route the signal to a different port. The optimization of each state was performed by searching for the peak of the optical power at the corresponding output port with respect to the bias voltages of the phase shifters iteratively. Since the carrier-induced phase modulation efficiency was lower than our design for this particular device, we also employed the reverse-bias-based electrooptic effect in combination with the forward-bias-based carrier injection [8]. The voltages applied to the phase shifters were between $-10$ and $+1.5$ V. Throughout the experiments, the input polarization state was maintained in the transverse-electric (TE) mode and the temperature of the device was maintained at 20 °C.

The static characteristics of the switch were measured in the 1530- to 1565-nm band ($C$-band). Fig. 2 shows the fiber-to-fiber transmissivity to the outputs (O1–O16) versus wavelength in all the switching states (S1–S16). In all the states, the wavelength dependence of the transmitted power is below 0.8 dB in the entire $C$-band. At the wavelength of 1550 nm, the static extinction ratio (the ratio of the Output $k$ power in State $k$ to the Output $k$ power in the other states) has an average value of 18.6 dB. The minimum extinction ratio is observed at Output 9 (S9/S8) and is equal to 11.3 dB. The fiber-to-fiber loss is between 15.1 dB (S11) and 17.0 dB (S1), out of which approximately 10 dB is estimated to be due to the fiber coupling. The on-chip loss is cross-checked from the Fabry–Pérot oscillation in the transmitted power spectrum caused by the lack of antireflection coating on the facets. The peak-to-valley ratio of these oscillations is above 1.5 dB, from which we calculate the

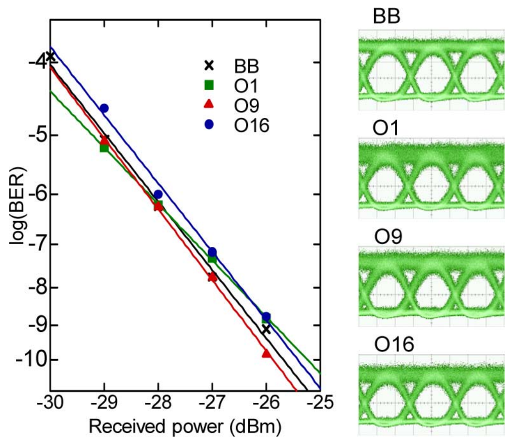


Fig. 3. BER of 40-Gb/s NRZ-OOK PRBS transmitted through the switch at S1, S9, and S16 compared to the back-to-back (BB) configuration, and the corresponding eye diagrams.

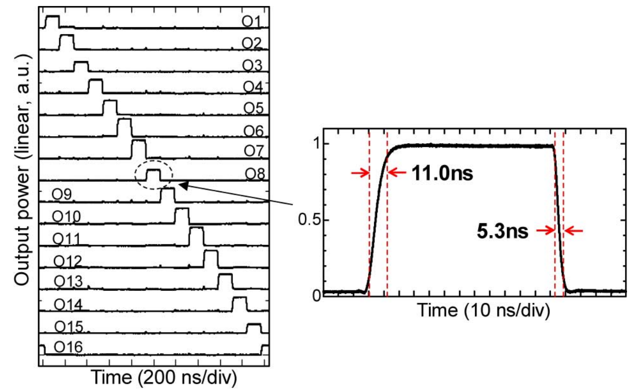


Fig. 4. Time-domain waveforms at the outputs (O1-O16) while the switch dynamically traces all of the states (S1-S16), and the enlarged view of the transition S7-S8-S9 (inset).

on-chip loss to be less than 7 dB in all of the switching states. We improved the on-chip loss by 11 dB compared to our previously reported $1 \times 8$ switch [8] by removing the absorptive p-InGaAs contact layer in the passive sections and mitigating the sidewall roughness of the waveguides. The residual power nonuniformity of 1.9 dB among the output ports may be reduced by appropriate apodization of the width of the arrayed waveguides.

We characterized the power penalty of the switch under static conditions. A 40-Gb/s nonreturn-to-zero (NRZ) on–off-keyed (OOK) pseudorandom bit sequence (PRBS) with a length of $2^7-1$ bits was transmitted through the switch to measure the bit-error rate (BER) in a preamplified receiver configuration. Fig. 3 shows the BERs measured at S1, S9, and S16. Owing to the all-passive configuration, the switch is fundamentally noiseless and the power penalty is below 0.4 dB at the BER of $10^{-9}$.

Finally, we operated the device in the dynamic switching mode using a specially developed switch driver circuit, consisting of field-programmable gate arrays (FPGAs) and digital-to-analog converters. The driver is capable of generating 24 synchronous analog voltages according to the 4-bit digital control signal representing the switching state. The voltage settings of the 16 states are saved in a look-up-table in the FPGA and are rewritable depending on the conditions of the switch. Fig. 4 displays the time-domain waveforms at the outputs in a representative scenario, in which the switch traces all the states from S1 to S16 sequentially. The dynamic extinction ratio is larger than 10.9 dB at all the outputs. Although there is a residual crosstalk observed during transitions, it may have limited impact in a typical OPS application with sufficient guard times. The inset shows the magnified view of the waveform at O8 during the S7–S8–S9 transition. The rise and fall times (10%–90%) are 11.0 and 5.4 ns, respectively. This response time is attributed to the carrier lifetime, device parasitics, and dynamic response of the driver circuit. Similar dynamic characteristics were also observed with different randomly selected orders of switching states.

## IV. Conclusion

A monolithically integrated InP $1 \times 16$ optical phased-array switch has been characterized for broadband WDM-OPS application. We have achieved static switching with a wavelength dependence of less than 0.8 dB in the entire $C$-band, low-penalty transmission of 40-Gb/s NRZ signal, and complete dynamic switching with reconfiguration times below 11 ns. This wavelength-insensitive high-speed optical switch can potentially be used to switch multiterabit/second WDM optical packets with relatively low power consumption, size, and cost.

## References


[1] D. J. Blumenthal, “Optical packet switching,” in *Proc. IEEE Lasers and Electro-Optics Society Annual Meeting*, Nov. 2004, vol. 2, pp. 910–912.

[2] H. Furukawa, N. Wada, N. Takezawa, K. Nashimoto, and T. Miyazaki, “640 $(2 \times 32\lambda \times 10)$ Gbit/s polarization-multiplexed, wide-colored optical packet switching achieved by polarization-independent high-speed PLZT switch,” in *Proc. Optical Fiber Communication Conf.*, San Diego, CA, 2008, Paper OTuL7.

[3] T. Tanemura, K. Takeda, and Y. Nakano, “Wavelength-multiplexed optical packet switching using InP phased-array switch,” *Opt. Express*, vol. 17, no. 11, pp. 9454–9459, May 2009.

[4] S. Nagarajan *et al.*, “Single-chip 40-channel InP transmitter photonic integrated circuit capable of aggregate data rate of 1.6 tbit/s,” *Electron. Lett.*, vol. 42, no. 13, pp. 771–773, Jun. 2006.

[5] R. M. Jenkins, J. M. Heaton, D. R. Wight, J. T. Parker, J. C. H. Birbeck, G. W. Smith, and K. P. Hilton, “Novel $1 \times N$ and $N \times N$ integrated optical switches using self-imaging multimode GaAs/ALGaAs waveguides,” *Appl. Phys. Lett.*, vol. 64, no. 6, pp. 684–686, Feb. 1994.

[6] Y. Kai, K. Sone, S. Yoshida, Y. Aoki, and G. N. Kinoshita, “A compact and lossless $8 \times 8$ SOA gate switch subsystem for WDM optical packet interconnections,” in *Proc. Eur. Conf. Optical Communication*, Brussels, Belgium, 2008, Paper We.2.D.4.

[7] T. Tanemura, M. Takenaka, A. A. Amin, K. Takeda, T. Shioda, M. Sugiyama, and Y. Nakano, “InP–InGaAsP integrated $1 \times 5$ optical switch using arrayed phase shifters,” *IEEE Photon. Technol. Lett.*, vol. 20, no. 12, pp. 1063–1065, Jun. 15, 2008.

[8] I. M. Soganci, T. Tanemura, and Y. Nakano, “Integrated $1 \times 8$ optical phased-array switch with low polarization sensitivity for broadband optical packet switching,” *IEEE Photonics J.*, vol. 1, no. 2, pp. 80–87, Aug. 2009.

[9] I. M. Soganci *et al.*, “Integrated phased-array $1 \times 16$ photonic switch for WDM optical packet switching application,” in *Proc. Int. Conf. Photonics in Switching*, Pisa, Italy, 2009, Paper WeI3.

[10] T. Tanemura and Y. Nakano, “Design and scalability analysis of optical phased-array $1 \times N$ switch on planar lightwave circuit,” *IEICE Electron. Express*, vol. 5, no. 16, pp. 603–609, Aug. 2008.